Applied Radiation and Isotopes 106 (2015) 68–71

Contents lists available at ScienceDirect

Applied Radiation and Isotopes

journal homepage: www.elsevier.com/locate/apradiso

Near threshold ^{7}Li(p,n) ^{7}Be reaction as neutron source for BNCT

D.M. Minsky [a,b,c,*], A.J. Kreiner [a,b,c]

[a] Gerencia de Investigación y Aplicaciones, CNEA, Av. Gral Paz 1499 (B1650KNA), San Martín, Buenos Aires, Argentina
[b] Escuela de Ciencia y Tecnología, UNSAM, M. de Irigoyen 3100 (1650), San Martín, Argentina
[c] CONICET, Av. Rivadavia 1917 (C1033AAJ), Buenos Aires, Argentina

HIGHLIGHTS

- Near threshold ^{7}Li(p,n)^{7}Be has been analyzed for BNCT.
- Good tumor doses can be obtained in less than 60 min of irradiation time.
- Undesirable effects of the unavoidable ^{7}Li(p,γp')^{7}Li gamma has been minimized.
- Doses to tumor up to ~55 Gy-Eq have been obtained.
- Beam currents as low as 3 mA can deliver 40 Gy-Eq to tumor.

ARTICLE INFO

Article history:
Received 30 January 2015
Received in revised form
26 June 2015
Accepted 25 July 2015
Available online 28 July 2015

Keywords:
Boron Neutron Capture Therapy (BNCT)
Neutron Sources
Near Threshold 7Li(p,n)7Be reaction

ABSTRACT

^{7}Li(p,n)^{7}Be is an endothermic reaction and working near its threshold (1.88 MeV) has the advantage of neutron spectra with maximum energies of about 100 keV, considerably lower than at higher beam energies, or than using other neutron-producing reactions or as for the uranium fission spectrum, relevant for BNCT based on nuclear reactors. With this primary energy it is much easier to obtain the energies needed for treating deep seated tumors by BNCT (about 10 keV). This work studies bombarding energies up to 2.05 MeV, different beam incidence angles and the effect of the undesirable gamma production via the ^{7}Li(p,γp') ^{7}Li reaction.

1. Introduction

The near threshold use of the ^{7}Li(p,n)^{7}Be reaction has been proposed and studied as a neutron source for Boron Neutron Capture Therapy (BNCT) (Tanaka et al., 2004). Since this reaction is endothermic, the emitted neutron energy can be modulated with the proton bombarding energy. As the neutron energy gets down to the order of tens of keV, they can be easily moderated but the neutron yield also decreases. The optimal energy should be a balance of these two facts. At this energy regime, neutron energy depends drastically on the emerging angle, so the bombarding angle is studied as an optimization parameter. The irradiation angle has not been previously studied and can lead to treatment improvements.

The unavoidable ^{7}Li(p, p'γ) ^{7}Li reaction in the same target produces undesirable 478 keV gamma radiation that gives non-specific dose to the patient. This contribution can be reduced by the correct choice of the target thickness.

This work has been carried out in the framework of the development of an accelerator devoted to BNCT within our group (Kreiner et al., 2011).

2. Materials and methods

2.1. Reaction yield calculation

The generation of the neutrons is based on the reaction of protons on a metallic lithium target. A code developed for previous work has been used. The double differential neutron yield per solid angle and energy has been calculated following Lee and Zhou (1999), but based on more recent cross section data. For further details on the cross section data refer to Minsky et al. (2011). A 2D matrix consisting in the discretized double differential neutron yield every 1° and 1 keV is generated with this code. These neutron yields are used as an input for Monte Carlo simulations. This article explores a bombarding region not previously studied: from 1.925 MeV up to 2.05 MeV.

---

[*] Corresponding author at: Gerencia de Investigación y Aplicaciones, CNEA, Av. Gral Paz 1499 (B1650KNA), San Martín, Buenos Aires, Argentina. Fax: +54 11 6772 7121.
E-mail address: minsky@tandar.cnea.gov.ar (D.M. Minsky).

http://dx.doi.org/10.1016/j.apradiso.2015.07.038
0969-8043/

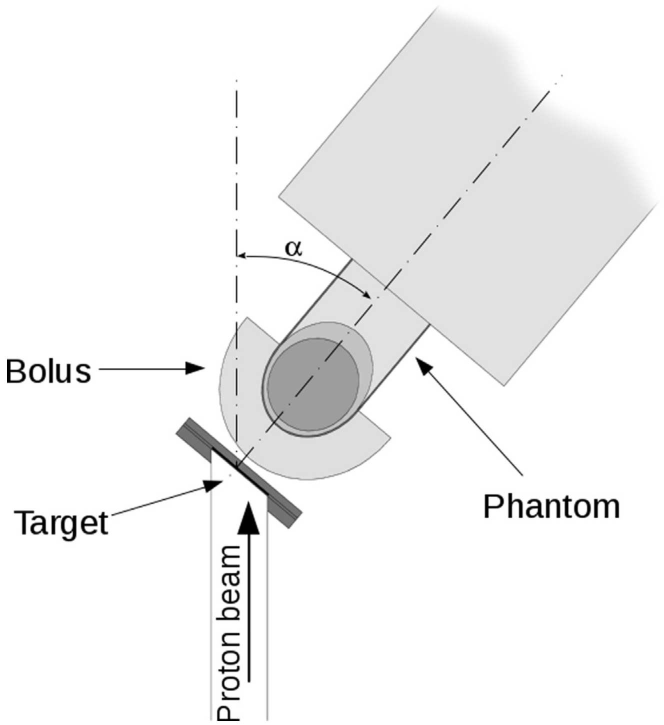

Fig. 1. Beam shaping assembly design.

Table 1
Weight factors assumed for dose calculations.

Tissue	γ RBE	Neutron RBE	^{10}B CBE	^{10}B Concentration [ppm]
Healthy brain	1	3.2	1.3	15
Skin	1	3.2	2.5	22.5
Tumor	1	3.2	3.8	52.5

Table 2
Prescriptions for the treatment session.

Maximum healthy brain punctual dose	11 Gy-Eq
Maximum skin dose	16.7 Gy-Eq
Maximum healthy brain mean dose	7 Gy-Eq
Maximum irradiation time	60 min

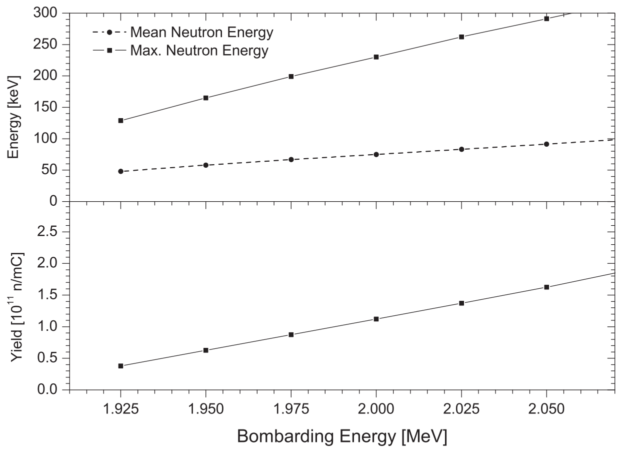

Fig. 2. Neutron yields and characteristic energies for each proton bombarding energy.

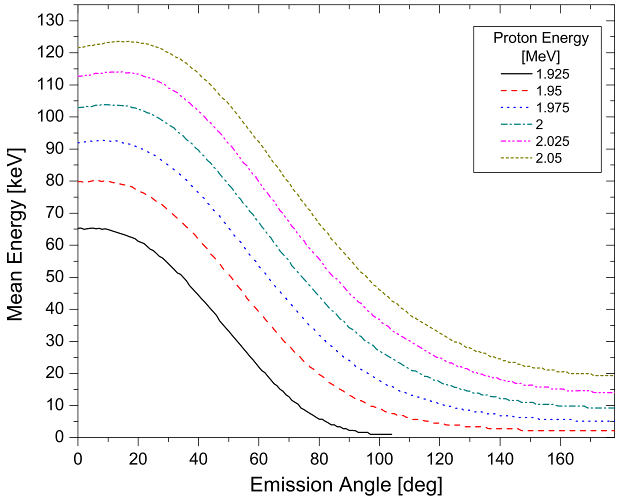

Fig. 3. Neutron mean energy as function of emission angle for each proton bombarding energy.

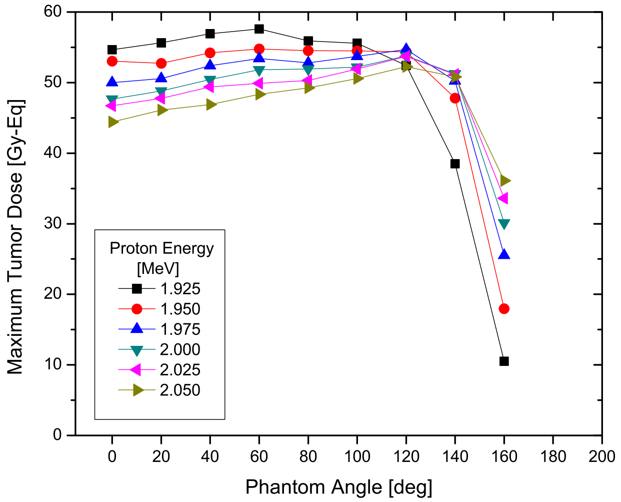

Fig. 4. Maximum tumor dose for different proton energies as function of the phantom angle.

2.2. Irradiation scheme and dose simulations

A complete metallic lithium target with its cooling system has been considered (Fig. 1). The cooling system is located in the back of the target and consists of a set of micro-channels where refrigerating water circulates (details not shown). The importance of considering the full target is that it has an important role as moderator in the low energy regime. Other studies made on the same energy regime lack the inclusion of the target cooling system and hence may be not reliable. The beam radius is 4.5 cm, thus the neutron source consists in a small disk which results in an effect equivalent to a small collimated port. A Snyder head phantom (Goorley, 2002) was positioned at different angles (α) with respect to the beam direction. A bolus material of A-150 plastic loaded with 10% in mass, 95% enriched ^{6}Li carbonate was used as a moderator and thermal neutron shield.°

MCNP5 (Brown et al., 2002) simulations have been made considering bombarding energies from 1.925 MeV up to 2.05 MeV in 0.025 MeV steps, phantom angles from 0 to 160° in 20° steps and bolus thickness from 0.25 cm up to 7 cm in 0.5 cm steps. Depth dose profiles along the phantom axis have been computed. ICRU 46 (1992) tissue compositions have been considered. Assumed relative biological effectiveness factors (RBEs), compound biological effectiveness

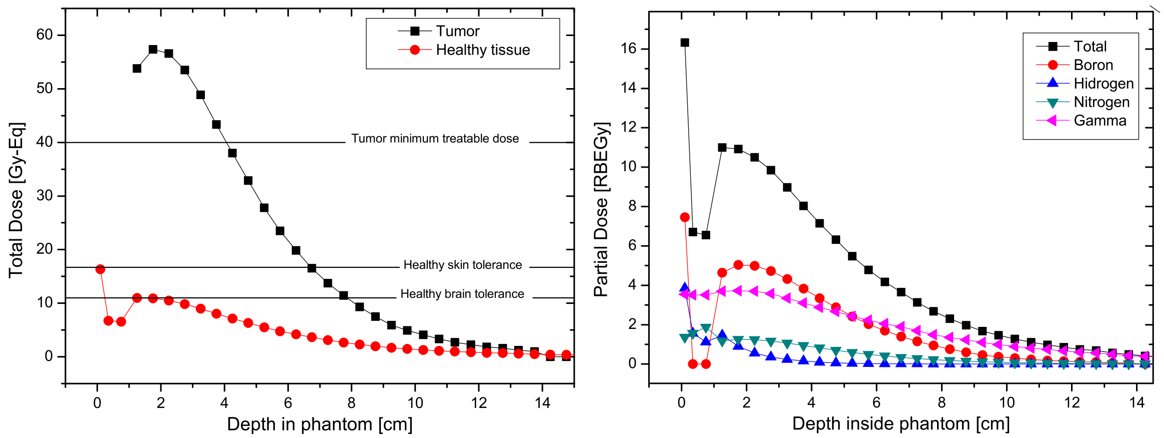

Fig. 5. Depth dose profiles for the optimal configuration with bombarding energy of 1.925 MeV. Left: Healthy tissue and tumor doses. Right: Healthy tissue components.

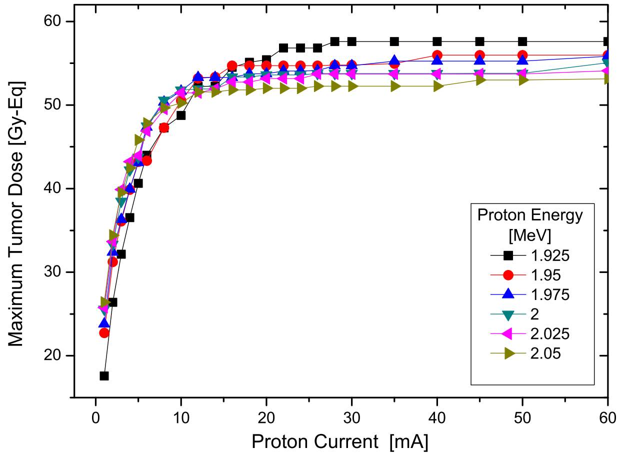

Fig. 6. Maximum tumor dose that can be obtained for different beam.

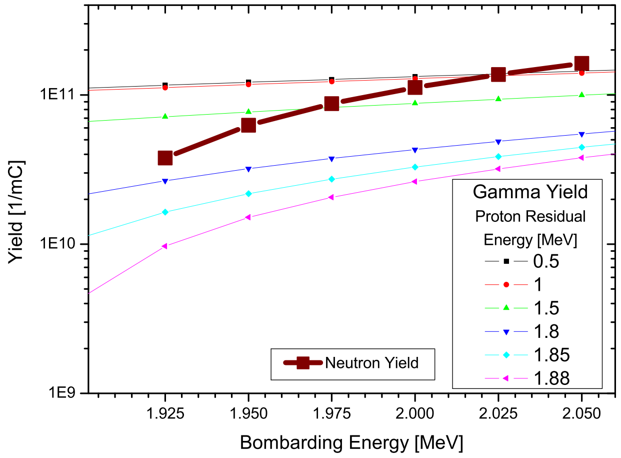

Fig. 7. Gama yield of ^{7}Li(p,p′γ)^{7}Li reaction for different target thicknesses compared to ^{7}Li(p,n)^{7}Be neutron yield.

factors (CBEs), boron concentrations and dose prescriptions are taken from Minsky and Kreiner (2014) and shown in Tables 1 and 2.

The optimization criteria were to maximize the punctual tumor dose at the depth that maximizes the depth dose profile while maintaining the dose to healthy tissues under the prescription tolerance and maximum irradiation time. For a defined bombarding energy, the parameters to optimize are the bolus thickness and the irradiation angle.

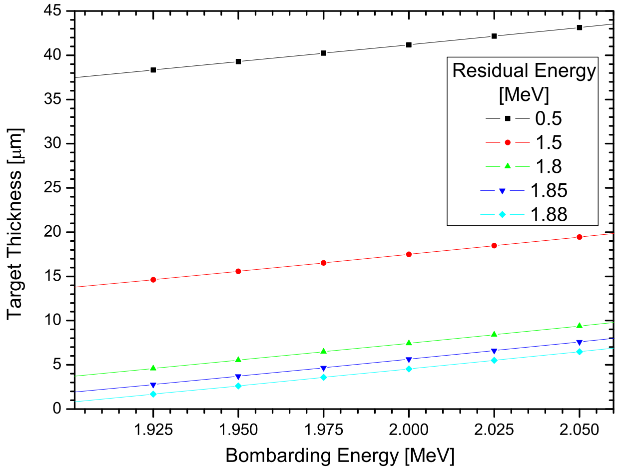

Fig. 8. Target thicknesses for various proton residual energies as function of bombarding energy.

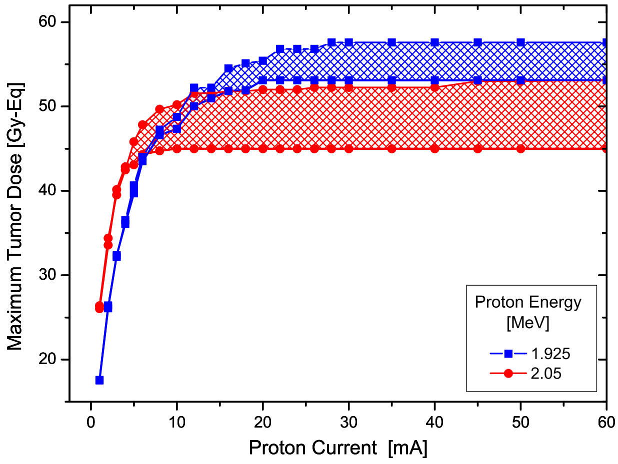

Fig. 9. Maximum tumor dose as function of proton current with and without considering the ^{7}Li(p,γp′)^{7}Li gamma production. This graph shows that the increase in the healthy tumor dose rate due to these gammas forces one to reduce the irradiation time and thus the tumor dose is reduced. For each bombarding energy, the upper curve is without considering the gamma contribution and the lower curve considering it.

2.3. Li(p,γp′)^{7}Li gamma production effect

The ^{7}Li(p,γp′)^{7}Li gamma ray producing reaction, that inevitably occurs in the target, has a much lower threshold energy than the ^{7}Li(p,n)^{7}Be neutron production reaction (0.478 MeV vs. 1.88 MeV). An option for minimizing this gamma production is with a target that is thin for this reaction but thick for the neutron production to avoid a reduction in the neutron yield. This means that the proton residual energy should be as close to the neutron production threshold as possible. This is possible with a solid target as the one considered here, but very difficult if not impossible with a liquid target.

Gamma ray productions for different bombarding energies and target thicknesses have been calculated from Mateus et al. (2002) cross sections and their effects have been calculated by MCNP simulations and added to the neutron beam effect.

3. Results

3.1. Neutron source

Neutron yields and characteristic energies for each proton bombarding energy are shown in Fig. 2. Neutron yield increases with bombarding energy which is in principle a positive fact, but the characteristic energies of the neutron also increase which should be as low as possible. At the near threshold energy regime, the neutron spectra have a strong angular dependence. As an example the mean energy as function of emission angle is shown in Fig. 3 for the analyzed bombarding energies.

3.2. Dose optimization

The optimization process consists in maximizing the maximum tumor dose. A 30 mA proton beam has been considered. Fig. 4 shows the optimized maximum tumor dose for different proton energies as function of the phantom angle. For each angle and proton energy combination the bolus thickness is the optimized parameter. This figure shows that the best angular position is not the forward direction, and for instance for 1.925 MeV protons the tumor dose is maximized at 60°.

As an example, Fig. 5 shows the depth dose profiles for the optimal case at 1.925 MeV bombarding energy. This case corresponds to a 4.75 cm thickness bolus and an irradiation angle of 60°.

The beam current is a critical aspect of the accelerator design. An analysis of the maximum tumor dose that can be obtained for different beam currents is shown in Fig. 6. Tumor doses above 40 Gy-Eq can be obtained with proton currents as low as 3 mA. With low currents the limiting factor is the irradiation time, thus non optimal small bolus thickness are used that do not maximize the tumor to healthy tissue dose rate ratio. The curves saturate at the current where the time is not the most limiting factor, thus the bolus thickness is optimal for maximizing this ratio. Higher currents will only benefit in a reduction in treatment time as the bolus thickness is already optimal.

The best configuration for each energy considering a beam current of 30 mA has an advantage depth in the range of 7.6–8.1 cm.

3.3. ^{7}Li(p,γp′)^{7}Li gamma production effect

Fig. 7 shows the neutron and gamma yield for different proton residual energies. In the case of a thick target the gamma production is even higher than the neutron production. The corresponding target thicknesses are shown in Fig. 8.

Even with a target thin enough so that the residual proton energy is 1.85 MeV and the gamma production is minimized, the irradiation time must be reduced in a small amount because of the extra gamma dose rate to healthy tissues. Thus, the tumor dose is reduced. Fig. 9 shows the reduction in the maximum tumor dose for two bombarding energies and a residual proton energy of 1.85 MeV. The tumor doses considering the ^{7}Li(p,p′γ) reaction are complete optimizations independent from the previous ones, thus for the same bombarding energy and beam current the angle of irradiation and bolus thickness may be different. The important effect of the gammas produced in the lithium has not been highlighted before, and shows the need to study dedicated gamma shieldings.

The maximum tumor dose for the best configuration and for a 30 mA current in the case of not considering the gamma production is 57.6 Gy-Eq, just a bit higher than the 56.7 Gy-Eq obtained in a previous work at the near resonance bombarding energy and with a Beam Shaping Assembly (Minsky and Kreiner, 2014). Considering this gamma component the best configuration can deliver up to 53.1 Gy-Eq. The Treatable Protocol Depth (TPD) for the best configuration according to the prescription on the present work is 4.41 cm, very similar to that reported by Kobayashi et al. (2007). However, if the criterion is to maximize the TPD, a TPD of 6.7 cm can be obtained but with a maximum tumor dose of 37 Gy-Eq, demonstrating that both criteria are not equivalent.

4. Conclusions

The near threshold ^{7}Li(p,n)^{7}Be reaction has been studied as a neutron source for BNCT. Satisfactory tumor doses can be obtained in this regime. This article shows that the patient should be positioned out of the beam axis to maximize the tumor dose. The effect of the gamma-producing ^{7}Li(p,γp′)^{7}Li unavoidable reaction in the target reduces the maximum obtainable tumor dose. This gamma component can be minimized by the use of a target thickness for which the residual proton energy is about the neutron production reaction threshold.

References

Brown, F., et al., 2002. MCNP version 5. Tech. rep. LA-UR-02-3935. Los Alamos National Laboratory Reports.

Goorley, J.T., 2002. Reference dosimetry calculations for neutron capture therapy with comparison of analytical and voxel models. Med. Phys. 29 (2), 145–156.

ICRU 46, 1992. Photon, electron, proton and neutron interaction data for body tissues. International Commission on Radiation Units and Measurements (Tech. Rep.).

Kobayashi, T., et al., 2007. Variations in lithium target thickness and proton energy stability for the near-threshold ^{7}Li(p,n)^{7}Be accelerator-based BNCT. Phys. Med. Biol. 52, 645–658.

Kreiner, A.J., et al., 2011. Development of a tandem-electrostatic-quadrupole facility for accelerator-based boron neutron capture. Ther. Appl. Radiat. Isot. 2011 (69), 1672–1675, and references therein.

Lee, C.L., Zhou, X.L., 1999. Thick target neutron yields for the ^{7}Li(p,n)^{7}be reaction near threshold. Nucl. Inst. Methods B 152 (1), 1–11.

Mateus, R., et al., 2002. Proton-induced γ-ray analysis of lithium in thick samples. Nucl. Inst. Method B 190 (1-4), 117–121.

Minsky, D., et al., 2011. AB-BNCT beam shaping assembly based on ^{7}Li(p,n)^{7}Be reaction optimization. Appl. Radiat. Isot. 69, 1668–1671.

Minsky, D.M., Kreiner, A.J., 2014. Beam shaping assembly optimization for ^{7}Li(p,n)^{7}Be accelerator based BNCT. Appl. Radiat. Isot. 88, 233–237.

Tanaka, K., et al., 2004. Characteristics of BDE dependent on ^{10}B concentration for accelerator-based BNCT using near-threshold ^{7}Li(p,n)^{7}Be direct neutrons. Appl. Radiat. Isot. 2004 (61), 875–879.